A Toeplitz Formulation of a Real-Time Algorithm for Time Decoding Machines *

Aurel A. Lazar, Ernő K. Simonyi and László T. Tóth

November 5, 2005

Abstract

Time encoding is a real-time asynchronous mechanism for encoding the amplitude information of an analog bandlimited signal into a time sequence, or time codes, based on which the signal can be reconstructed. Using a Toeplitz formulation we propose an efficient real-time reconstruction procedure. As an illustration, time encoding is carried out by an asynchronous sigma-delta modulator. The proposed method is confirmed by numerical simulations.

1 Introduction

Time-encoding is a real-time asynchronous mechanism of mapping the amplitude information of a bandlimited signal $x(t)$, $t \in \mathbb{R}$, into a set of time codes (TCs) $\{t_k\}$, $k \in \mathbb{Z}$, where $\mathbb{R}$ and $\mathbb{Z}$ denote the sets of real numbers and integers, respectively. The TCs are generated by Time Encoding Machines (TEMs) driven by $x(t)$. The TEMs are simple nonlinear asynchronous analog circuits with typically low power consumption. Usually the TEM output, $z(t)$, is an asynchronous binary signal or pulse-train based on which the TCs can be identified.

Known nonlinear asynchronous analog circuits can be used as TEMs. The first example of a TEM (see [9] and the references therein), also shown in Fig. 1, was an asynchronous sigma-delta modulator. Other TEMs include integrate-and- fire neurons [10] and frequency modulators [11]. Based on the TCs, $x(t)$ can be reconstructed by algorithms commonly referred to as Time Decoding Machines (TDMs) if certain Nyquist-type rate conditions on the TCs are met. Although methods used in frame theory [2, 8] and irregular sampling [4, 15] are needed to establish these conditions [11, 10], the algorithms are often easy to find and are reduced to solving consistent but (typically) ill-conditioned set of linear equations.

*BNET Technical Report #6-05, Department of Electrical Engineering, Columbia University, New York, NY, October 2005. Proceedings of the Conference on Telecommunication Systems, Modeling and Analysis, Dallas, TX, November 17-20, 2005, to appear.

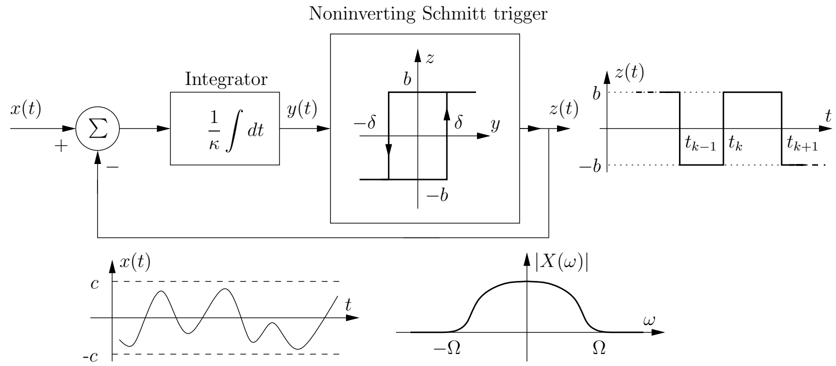

Figure 1: Asynchronous sigma-delta modulator as a TEM.

The first example of a TEM [9, 11] was an asynchronous sigma-delta modulator [7, 14] shown in Figure 1. The TEM consists of integrator and a symmetrically-centered noninverting Schmitt trigger in a negative-feedback arrangement where κ, δ and b are circuit parameters. As shown, the zero-crossings of the asynchronous binary output $z(t)$ define the TCs. Furthermore, the input signal is bounded both in amplitude and (angular) frequency as

$$|x(t)| \leq c < b \quad \text{and} \quad X(\omega) = 0 \text{ if } |\omega| < \Omega, \tag{1}$$

where $X(\omega)$ denotes the Fourier transform of $x(t)$.

The operation of this TEM is simple. Since $z(t)$ takes either b or $-b$ values, the input to the integrator is either $x(t) + b$ or $x(t) - b$. Since $|x(t)| \leq c < b$, the integrator output $y(t)$ is a strictly increasing or decreasing function for $t \in (t_k, t_{k+1})$ and thus either $y(t_k) = \delta$ or $y(t_k) = -\delta$. A simple analysis [11] gives

$$\int_{t_k}^{t_{k+1}} x(t)dt = (-1)^k(2\kappa\delta - b(t_{k+1} - t_k)) \tag{2}$$

for all $k \in \mathbb{Z}$. The original TDM of [9] can be found by assuming that $x(t)$ is expressed as

$$x(t) = \sum_{\ell\in\mathbb{Z}} c_\ell g(t - s_\ell), \quad s_\ell = \frac{t_\ell + t_{\ell+1}}{2}, \quad \text{and} \quad g(t) = \frac{\sin(\Omega t}{\pi t} \tag{3}$$

is the impulse response of an ideal lowpass filter (LPF) with cutoff frequency Ω. The goal is to find the coefficients c_ℓ. Substituting (3) into (2) gives:

$$\sum_{\ell\in\mathbb{Z}} \underbrace{c_\ell}_{[\mathbf{c}]_\ell} \underbrace{\int_{t_k}^{t_{k+1}} g(t - s_\ell)dt}_{[\mathbf{G}]_{k,\ell}} = \underbrace{(-1)^k(2\kappa\delta - b(t_{k+1} - t_k))}_{[\mathbf{q}]_k}. \tag{4}$$

With the definitions of the matrix $\mathbf{G}$ and, vectors $\mathbf{q}$ and $\mathbf{c}$ introduced in (4), the unknown $\mathbf{c}$ verify the linear equations $\mathbf{Gc} = \mathbf{q}$. It can be shown [11] that this formulation gives perfect reconstruction if the condition $2\kappa\delta/(b - c) < \pi/\Omega$ is satisfied. Note that $\mathbf{G}$, $\mathbf{q}$ and $\mathbf{c}$ have infinite dimensions.

1.1 Toeplitz Formulation

In the case of irregular sampling, an efficient approximation was proposed by transforming the linear equations $\mathbf{Gc} = \mathbf{q}$ into a system represented by a Hermitian Toeplitz matrix [5]. This approach was generalized to time encoding in [12] in two steps.

In the first step a reformulation of the reconstruction technique of Section 1 is introduced. If $x(t)$ is Ω- bandlimited, then so is its indefinite integral and therefore similarly to (3) as:

$$\int_{-\infty}^{t} x(u)du = \sum_{\ell \in \mathbb{Z}} c_\ell g(t - t_\ell), \tag{5}$$

where the c_ℓ's are to be determined. Subtracting (5) evaluated at $t = t_k$ from the same evaluated at $t = t_{k+1}$ gives:

$$\int_{t_k}^{t_{k+1}} x(u)du = \sum_{\ell \in \mathbb{Z}} c_\ell \left(g(t_{k+1} - t_\ell) - g(t_k - t_\ell) \right).$$

Using (2) and rewriting the left-hand-side (LHS) using Kronecker's notation gives:

$$\underbrace{(-1)^k (2\kappa\delta - b(t_{k+1} - t_k))}_{[\mathbf{q}]_k} = \sum_{\ell \in \mathbb{Z}} \underbrace{c_\ell}_{[\mathbf{c}]_\ell} \sum_{m \in \mathbb{Z}} \underbrace{g(t_m - t_\ell)}_{[\mathbf{G}]_{m,\ell}} \underbrace{(\delta_{k+1,m} - \delta_{k,m})}_{[\mathbf{P}]_{k,m}}$$

Using the matrices and vectors introduced above gives

$$\mathbf{q} = \mathbf{PGc},$$

or, equivalently

$$\mathbf{P}^{-1}\mathbf{q} = \mathbf{Gc}, \tag{6}$$

where

$$[\mathbf{P}^{-1}]_{\ell,k} = \begin{cases} -1 & \text{if} \quad \ell \leq k \\ 0 & \text{if} \quad \ell > k. \end{cases} \tag{7}$$

In the second step an approximation for $g(t)$ introduced in (3) is given by:

$$g(t) \simeq \alpha \sum_{n=-N}^{N} e^{jn\frac{\Omega}{N}t} = \alpha \frac{\sin\left(\frac{(2N+1)}{2N}\Omega t\right)}{\sin\left(\frac{\Omega t}{2N}\right)} \text{ with } \alpha = \frac{\Omega}{(2N+1)\pi}. \tag{8}$$

When N tends to infinity this function converges to $g(t)$. At the same time, the approximating function is both Ω-bandlimited and periodic with a period $2N\pi/\Omega$.

Substituting (8) into (5) gives the approximation

$$\begin{aligned} \int_{-\infty}^{t} x(u)du &\simeq \sum_{\ell \in \mathbb{Z}} c_\ell \alpha \sum_{n=-N}^{N} e^{jn\frac{\Omega}{N}(t - t_\ell)} \\ &= \sum_{n=-N}^{N} e^{jn\frac{\Omega}{N}t} \underbrace{\alpha \sum_{\ell \in \mathbb{Z}} c_\ell e^{-jn\frac{\Omega}{N}t_\ell}}_{[\mathbf{d}]_n}. \end{aligned} \tag{9}$$

Defining the elements of the matrix $\mathbf{S}$ by

$$[\mathbf{S}]_{n,\ell} = e^{-jn\frac{\Omega}{N}t_\ell}, \tag{10}$$

the vector $\mathbf{d}$ introduced in (9) can be expressed as

$$\mathbf{d} = \alpha\mathbf{S}\mathbf{c}. \tag{11}$$

Taking the derivative of both sides of (9) gives the approximation

$$x(t) \simeq j\frac{\Omega}{N}\sum_{n=-N}^{N} n e^{jn\frac{\Omega}{N}t}[\mathbf{d}]_n \tag{12}$$

for $x(t)$. Note that the periodic approximation is a Fourier-series expansion with a finite number of coefficients. This suggests the use of the Fast Fourier Transform (FFT) as discussed in Section 2.6.

Based on equations (6) and (8), and given the definition of the vector $\mathbf{d}$ introduced in (9) we have

$$\begin{aligned}
[\mathbf{P}^{-1}\mathbf{q}]_k &= \sum_{\ell\in\mathbb{Z}}[\mathbf{G}]_{k,\ell}[\mathbf{c}]_\ell = \sum_{\ell\in\mathbb{Z}} g(t_k - t_\ell)c_\ell \\
&\simeq \sum_{\ell\in\mathbb{Z}} c_\ell \alpha \sum_{n=-N}^{N} e^{jn\frac{\Omega}{N}(t_k-t_\ell)} \\
&= \sum_{n=-N}^{N} e^{jn\frac{\Omega}{N}t_k}\alpha\sum_{\ell\in\mathbb{Z}} c_\ell e^{-jn\frac{\Omega}{N}t_\ell} = \sum_{n=-N}^{N} e^{jn\frac{\Omega}{N}t_k}[\mathbf{d}]_n
\end{aligned}$$

In matrix form

$$\mathbf{P}^{-1}\mathbf{q} \simeq \mathbf{S}^H\mathbf{d}, \tag{13}$$

where $\mathbf{S}$ was defined in (10) and superscript ^{H} denotes conjugate transposition. Introducing the diagonal matrix (see [12])

$$\mathbf{D} = \mathrm{diag}(t_{k+1} - t_k), \tag{14}$$

and multiplying both sides of (13) by $\alpha\mathbf{S}\mathbf{D}$ gives $\alpha\mathbf{S}\mathbf{D}\mathbf{P}^{-1}\mathbf{q} = \alpha\mathbf{S}\mathbf{D}\mathbf{S}^H\mathbf{d}$. As a result, with

$$\mathbf{T} = \alpha\mathbf{S}\mathbf{D}\mathbf{S}^H = \alpha\sum_{k\in\mathbb{Z}}(t_{k+1} - t_k)e^{j(m-n)\frac{\Omega}{N}t_k} \tag{15}$$

the set of linear equations

$$\alpha\mathbf{S}\mathbf{D}\mathbf{P}^{-1}\mathbf{q} = \mathbf{T}\mathbf{d} \tag{16}$$

needs to be solved for $\mathbf{d}$. Note that $\mathbf{P}^{-1}$ and α are given (see (7) and (8)), and $\mathbf{S}$, $\mathbf{D}$, $\mathbf{T}$ and $\mathbf{q}$ are determined by the TCs. Note also that $\mathbf{T}$ is a Hermitian Toeplitz matrix.

Therefore, instead of the exact reconstruction in (3) with corresponding linear equations $\mathbf{G}\mathbf{c} = \mathbf{q}$ represented by a not well structured matrix $\mathbf{G}$ (see (4)), we now have an approximate reconstruction in (12) together with the linear equations in (16) represented by a structured matrix $\mathbf{T}$. The "exact reconstruction" using infinite-dimensional vectors and matrices is most often intractable, and finite-dimensional matrices and vectors are used in practice.

2 The Proposed Real-Time TDM

Using the original reconstruction method of [11], also outlined in Section 1, a multiresolution algorithm is presented in [13] to stitch finite-dimensional approximations together by using appropriate window functions. We present below an alternative solution based on the Toeplitz formalism discussed in Section 1.1.

2.1 Finite Dimensional Covering

Our simulation experience shows that using the finite range $[t_k, t_\ell]$ with $k < \ell$, i.e. using the finite set of TCs $\{t_k, t_{k+1}, \ldots, t_\ell\}$, an accurate approximation can be achieved in a reduced range $[t_{k+M}, t_{\ell-M}]$ both for the original [11] and the Toeplitz-based reconstruction [12]. Here $M \in \mathbb{Z}$ typically ranges between 2 and 5. In particular, we define the finite-dimensional versions of the vectors and matrices introduced in Section 1.1 as:

$$\begin{aligned}
[\mathbf{q}_{k,\ell}]_{i-k+1} &= (-1)^i(2\kappa\delta - b(t_{i+1} - t_i)) \\
\mathbf{D}_{k,\ell} &= \mathrm{diag}(t_{i+1} - t_i) \\
[\mathbf{S}_{k,\ell,N}]_{n+N+1,i-k+1} &= e^{-jn\frac{\Omega}{N}t_i} \\
\left[\mathbf{P}^{-1}_{k,\ell}\right]_{r-k+1,i-k+1} &= \begin{cases} -1 & \text{if} \quad r \leq i \\ 0 & \text{if} \quad r > i \end{cases} \\
[\mathbf{T}_{k,\ell,N}]_{m+N+1,n+N+1} &= \alpha \sum_{i=k}^{\ell} (t_{i+1} - t_i) e^{j(m-n)\frac{\Omega}{N}t_i}
\end{aligned} \tag{17}$$

for all integers $i, r = k, \ldots, \ell$ and $m, n = -N, \ldots, N$. Then, the correspondence of the linear equations in (16) becomes

$$\alpha \mathbf{S}_{k,\ell,N} \mathbf{D}_{k,\ell} \mathbf{P}^{-1}_{k,\ell} \mathbf{q}_{k,\ell} = \mathbf{T}_{k,\ell,N} \mathbf{d}_{k,\ell,N}$$

for the unknown (finite-dimensional) vector $\mathbf{d}_{k,\ell,N}$. Since matrix $\mathbf{T}_{k,\ell,N}$ of size $(2N+1) \times (2N+1)$ can easily be ill-conditioned, a familiar (minimum-norm) solution is given by

$$\mathbf{d}_{k,\ell,N} = \alpha \mathbf{T}^{+}_{k,\ell,N} \mathbf{S}_{k,\ell,N} \mathbf{D}_{k,\ell} \mathbf{P}^{-1}_{k,\ell} \mathbf{q}_{k,\ell} \tag{18}$$

where $\mathbf{T}^{+}_{k,\ell,N}$ denotes the pseudo inverse of $\mathbf{T}_{k,\ell,N}$ [1]. Using the solution $\mathbf{d}_{k,\ell,N}$ in (12) gives

$$x_{k,\ell,N}(t) = j\frac{\Omega}{N} \sum_{n=-N}^{N} n e^{jn\frac{\Omega}{N}t} [\mathbf{d}_{k,\ell,N}]_n \tag{19}$$

as a Fourier-series approximation for $x(t)$ for $t \in [t_{k+M}, t_{\ell-M}]$ using finite number of coefficients.

2.2 A Multiresolution Algorithm for Signal Recovery

Consider the set of window functions, $w(t)$, forming a partition of unity

$$\sum_{n\in\mathbb{Z}} w(t - nT_0) = 1 \tag{20}$$

with some known period T_0. Several window functions of this type are available in the literature. For example, partition of unity is a requirement for so called *admissible scaling functions* in Wavelet Theory (see, e.g., [16, 3]). To simplify the analysis we assume that $w(t)$ is even and has a compact support, i.e., $w(t) = w(-t)$ and for some known T_w we have $w(t) = 0$ if $t \notin [-T_w, T_w]$. Here T_w is determined by T_0 depending on the (known) shape of $w(t)$ as illustrated Figure 2.

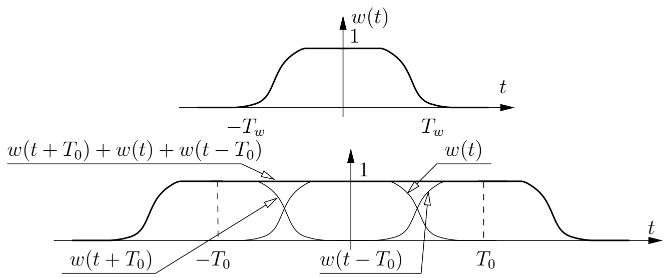

Figure 2: Illustration for the window function and the partition of unity.

Now, from the obvious relationship (see also (20))

$$x(t) = x(t)\sum_{n\in\mathbb{Z}} w(t - nT_0) = \sum_{n\in\mathbb{Z}} w(t - nT_0)x(t) \tag{21}$$

we can see (see also Figure 2) that

$$w(t - nT_0)x(t) = 0 \quad \text{for} \quad t \notin [nT_0 - T_w, nT_0 + T_w]$$

holds.

Therefore, if a good approximation of $x(t)$ can be achieved for $t \in [nT_0 - T_w, nT_0 + T_w]$, then no problem will arise if the approximation is not good for $t \notin [nT_0 - T_w, nT_0 + T_w]$. The approximation discussed in Section 2.1 can be matched to the window functions as illustrated in Figure 3. As shown, since the times $nT_0 - T_w$ are known, $k_n \in \mathbb{Z}$ and $\ell_n \in \mathbb{Z}$ are defined as:

$$\begin{array}{rclcccccc} k_n & := & \{t_{k_n} & \leq & nT_0 - T_w & \text{and} & t_{k_n+1} & > & nT_0 - T_w\} \\ \ell_n & := & \{t_{\ell_n-1} & \leq & nT_0 + T_w & \text{and} & t_{\ell_n} & > & nT_0 + T_w\}. \end{array} \tag{22}$$

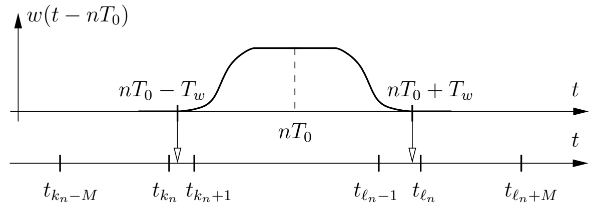

Figure 3: Illustration for matching the TCs to $w(t - nT_0)$.

Comparing this results with the formulation of Section 2.1 we have that $k = k_n - M$ and $\ell = \ell_n + M$. Therefore, with the notation of (19) the approximating signal corresponding to $w(t - nT_0)$ is given by:

$$x_{k_n-M,\ell_n+M,N}(t) = j\frac{\Omega}{N}\sum_{m=-N}^{N} me^{jm\frac{\Omega}{N}t}[\mathbf{d}_{k_n-M,\ell_n+M,N}]_m. \tag{23}$$

Substituting this relationship into (21) gives:

$$\sum_{n\in\mathbb{Z}} w(t-nT_0)j\frac{\Omega}{N}\sum_{m=-N}^{N} me^{jm\frac{\Omega}{N}t}[\mathbf{d}_{k_n-M,\ell_n+M,N}]_m.$$

Introducing

$$d(M,N)_{m,n} = m[\mathbf{d}_{k_n-M,\ell_n+M,N}]_m \tag{24}$$

gives the overall approximation for $x(t)$:

$$x_{M,N}(t) = \sum_{n\in\mathbb{Z}}\sum_{m=-N}^{N} d(M,N)_{m,n}w(t-nT_0)e^{jm\frac{\Omega}{N}t} \tag{25}$$

2.3 Example

With $c = 0.3$ and $\Omega = 2\pi \times 40$ krad/s, the input signal was created as a sum 20 sinusoids with amplitudes, frequencies, and phases randomly selected within $[-c, c]$, $[0, \Omega/2\pi]$, and $[0, 2\pi]$, respectively. In numerical simulations for the TEM in Figure 1, 123 TCs together with the signals shown were determined with high accuracy. The input signal $x(t)$, the integrator output $y(t)$, and the overall TEM output $z(t)$ are shown in Figure 4 ranging t from zero to 875.5 μs.
Using the settings

$$T_0 = T_w = \frac{2\pi}{\Omega},$$

the window functions were selected as:

$$w(t) = \begin{cases} \cos^2\left(\frac{\pi t}{2T_w}\right) & \text{if} \quad t \in [-T_w, T_w] \\ 0 & \text{if} \quad t \notin [-T_w, T_w] \end{cases}$$

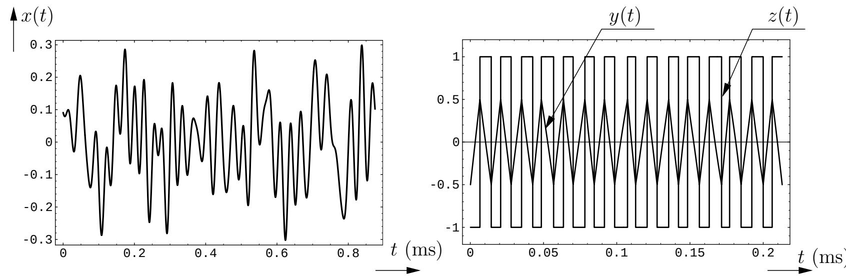

Figure 4: Simulated TEM signals, $x(t)$, $y(t)$ and $z(t)$ of Fig. 1.

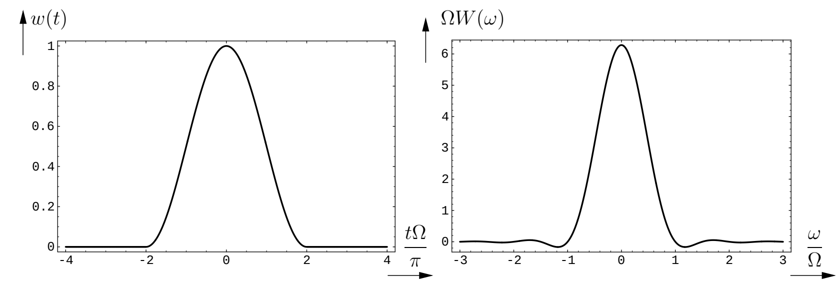

Figure 5: Normalized $w(t)$ and its Fourier transform $W(\omega)$.

Therefore the Fourier transform of $w(t)$ is given by

$$W(\omega) = \frac{\pi^2 \sin(\omega T_w)}{\pi^2 \omega - T_w^2 \omega^3}$$

Figure 5 shows $w(t)$ and $W(\omega)$ in scaled form. Two time-shifted window functions, $w(t - 10T_0)$ and $w(t - 22T_0)$, are also shown in Figure 6 in dashed gray line.

With (see Figure 3) $M = 5$ the proposed reconstruction procedure was implemented. Using the periodic functions in (23) simulation results are shown in Figure 6 for $N = 8$. It can be seen that $x_{26,44,8}(t)$ and $x_{68,86,8}(t)$ give good approximations for $t \in [nT_0 - T_w, nT_0 + T_w]$, but outside this range the periodic approximations are poor. However, this is not a problem since $w(t - nT_0) = 0$ hence $w(t - nT_0) x_{k_n - M, \ell_n + M, N}(t) = 0$ for $t \notin [nT_0 - T_w, nT_0 + T_w]$. In the figure, $\mathcal{E}_n$ denotes the root-mean-square (RMS) value of the error functions defined as $e_n(t) = x_{k_n - M, \ell_n + M, N}(t) - x(t)$ and evaluated over the support of $w(t - nT_0) = 0$, $t \in [nT_0 - T_w, nT_0 + T_w]$.

The quality of the overall reconstruction in (25) is quantified by the error function

$$e_{M,N}(t) = x_{M,N}(t) - x(t)$$

for $t \in [T_{\min}, T_{\max}]$. Here $T_{\max}$ and $T_{\min}$ are appropriate simulation-dependent bounds. The RMS value of $e_{M,N}(t)$ in [dB] is defined by:

$$\mathcal{E}_{M,N} = 10 \lg \left(\frac{\int_{T_{\min}}^{T_{\max}} e_{M,N}^2(t) dt}{T_{\max} - T_{\min}} \right)$$

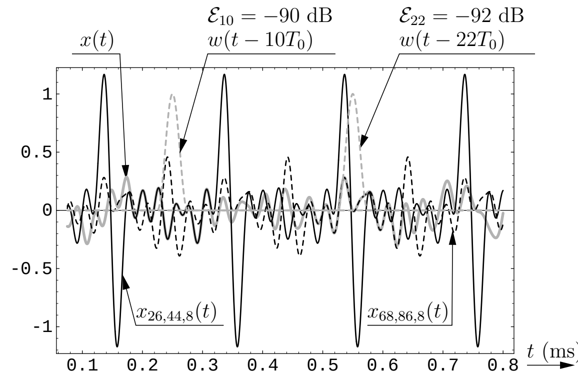

Figure 6: Approximating periodic functions given by (23) with $N = 8$.

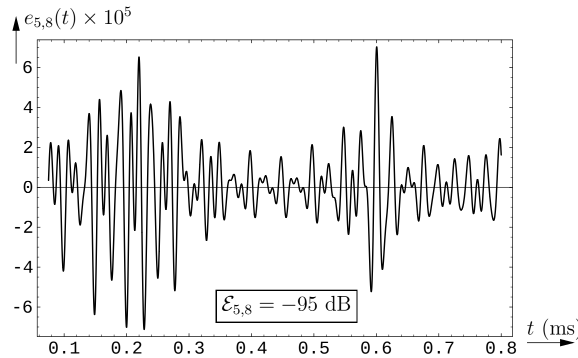

Figure 7: Scaled error function $e_{5,8}(t)$ with RMS value $\mathcal{E}_{5,8}$ evaluated using $T_{\min} = 75$ μs and $T_{\max} = 800$ μs.

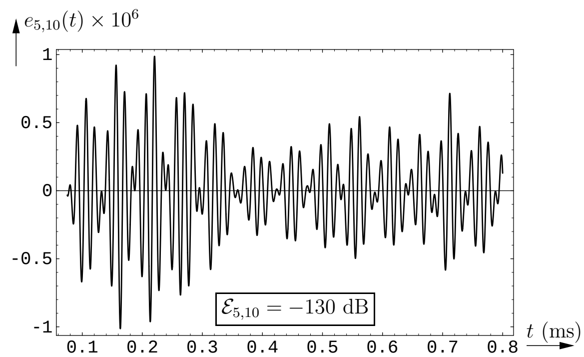

Figure 8: Scaled error function $e_{5,10}(t)$ with RMS value $\mathcal{E}_{5,10}$ evaluated using $T_{\min} = 75$ μs and $T_{\max} = 800$ μs.

Figure 7 shows $e_{5,8}(t)$ and $\mathcal{E}_{5,8}$ corresponding to the case $N = 8$, i.e., the case when the approximations in Figure 6 were obtained. The RMS error shows good agreement with those shown in Figure 6. Figure 8 shows $e_{5,10}(t)$ and $\mathcal{E}_{5,10}$ corresponding to the case $N = 10$.

Thus, increasing N, i.e., generating a better approximation for $g(t)$ in (8) increases the accuracy. However, the conditioning of the system matrices gets worse by increasing N [12]. The designer has a number of parameters to tune including the window width T_w, the window type, N, and M. Generally, increasing T_w requires larger value for N.

2.4 Postfiltering

The bandwidth of $x_{M,N}(t)$ certainly exceeds Ω. In particular, let Ω_w be such that $W(\omega) \simeq 0$ for $|\omega| > \Omega_w$. For example, with parameters of Section 2.3 using Figure 5, $\Omega_w = 3\Omega$ appears to be a safe choice. Since the bandwidth of $x_{k_n-M,\ell_n+M,N}(t)$ is Ω (see (23)), the bandwidth of the product $x_{k_n-M,\ell_n+M,N}(t)w(t-nT_0)$, and thus that of $x_{M,N}(t)$ is $\Omega + \Omega_w$. Using broader $w(t)$ in the time domain narrows $W(\omega)$ in the frequency domain, hence decreases Ω_u. However, with broader $w(t)$ more TCs are covered by $(nT_0 - T_w, nT_0 + T_w)$ which generally needs larger N. The enlarged size of the Toeplitz matrices $\mathbf{T}_{k_n-M,\ell+M,N}$ increases the computational load for calculating the pseudo inverses $\mathbf{T}^+_{k_n-M,\ell+M,N}$ in (18).

By appropriately choosing $w(t)$, Ω_w can be decreased for fixed T_w hence T_0. For example, if $w(t)$ is chosen as that in Figure 5, then both $w(t)$ and its derivative are continuous for all $t \in \mathbb{R}$. Then, as shown in Figure 5, a good enough frequency localization for $W(\omega)$ can be achieved.

Passing $x_{M,N}(t)$ through a lowpass filter with cutoff-frequency Ω restores the original bandwidth of the input signal. If digital signal processing is required on the reconstructed signal, the samples $x_{M,N}(nT_s)$, $T_s \geq \pi/(\Omega + \Omega_w)$, can be processed by a discrete-time LPF with (digital) cutoff frequency $\pi/(1 + \Omega_w/\Omega)$. Since the reconstruction error spreads over the range $\omega \in (-\Omega_w - \Omega, \Omega_w + \Omega)$, lowpass filtering in either analog or discrete-time domain further improves the overall accuracy [13].

2.5 Pseudo-Inverse Recursion

For a real-time TDM, the pseudo inversions $\mathbf{T}^+_{k,\ell,N}$ is a critical factor in terms of both computational complexity and accuracy. As in [13], instead of calculating $\mathbf{T}^+_{k_n-M,\ell_n+M,N}$ individually for each n, recursive solutions can be developed taking advantage of the fact that $\mathbf{T}_{k_n-M,\ell_n+M,N}$ and $\mathbf{T}_{k_{n+1}-M,\ell_{n+1}+M,N}$ have a number of common elements. One possible solution is based on the general result in [1] (page 50, Collorary 3.3.1):

$$\begin{aligned} \left(\mathbf{A} + \mathbf{u}\mathbf{v}^H\right)^+ &= \mathbf{A}^+ - \frac{1}{\beta}\mathbf{A}^+\mathbf{u}\mathbf{v}^H\mathbf{A}^+ \\ \text{where } \beta &= 1 + \mathbf{v}^H\mathbf{A}^+\mathbf{u} \neq 0 \end{aligned} \tag{26}$$

Thus, if an arbitrary matrix $\mathbf{A}$ is modified by a rank-one matrix, $\mathbf{u}\mathbf{v}^H$, then the pseudo inverse is also modified by a rank-one matrix, $(\mathbf{A}^+\mathbf{u})(\mathbf{v}^H\mathbf{A}^+)/\beta$.

Any matrix can be decomposed as a sum of rank-one matrices in several ways. For our

Toeplitz matrices

$$[\mathbf{T}_{k_n-M,\ell_n+M,N}]_{m+N+1,n+N+1} = \alpha \sum_{i=k_n-M}^{\ell_n+M} (t_{i+1}-t_i) e^{j(m-r)\frac{\Omega}{N}t_i}$$

with $m, r = -N. \ldots, N$ a decomposition as a sum of rank-one Hermitian matrices is possible after defining

$$[\mathbf{u}_i]_{r+N+1} = \sqrt{\alpha(t_{i+1}-t_i)} e^{-jr\frac{\Omega}{N}t_i}$$

with $r = -N, \ldots, N$ and $i = k_n - M, \ldots, \ell_n + M$ as:

$$\mathbf{T}_{k_n-M,\ell_n+M,N} = \sum_{i=k_n-M}^{\ell_n+M} \mathbf{u}_i \mathbf{u}_i^H. \tag{27}$$

Therefore for the "next" n (replacing n by $n+1$):

$$\mathbf{T}_{k_{n+1}-M,\ell_{n+1}+M,N} = \sum_{i=k_{n+1}-M}^{\ell_{n+1}+M} \mathbf{u}_i \mathbf{u}_i^H. \tag{28}$$

Since $k_{n+1} > k_n$ and $\ell_{n+1} > \ell_n$, combining (27) and (28) gives:

$$\mathbf{T}_{k_{n+1}-M,\ell_{n+1}+M,N} = \mathbf{T}_{k_n-M,\ell_n+M,N} + \sum_{i=\ell_n+M+1}^{\ell_{n+1}+M} \mathbf{u}_i \mathbf{u}_i^H - \sum_{i=k_n-M}^{k_{n+1}-M-1} \mathbf{u}_i \mathbf{u}_i^H.$$

Whenever a rank-one matrix $\mathbf{u}_i \mathbf{u}_i^H$ is added to or subtracted from $\mathbf{T}_{k_n-M,\ell_n+M,N}$, the result in (26) can be used recursively for calculating $\mathbf{T}^+_{k_{n+1}-M,\ell_{n+1}+M,N}$ in terms of $\mathbf{T}^+_{k_n-M,\ell_n+M,N}$. If for $n = 0$ some initial pseudo inverse $\mathbf{T}^+_{k_0-M,\ell_0+M,N}$ is given, then no further pseudo inversion is needed in the recursion for $n > 0$. Note however that, not even this initial pseudo inversion is needed if a short initial "transient" type of error can be tolerated in the overall reconstruction. Since in each recursion step new rank-one matrices are added and old rank-one matrices are subtracted, the "effect" of any initial value, say

$$\mathbf{T}_{k_0-M,\ell_0+M,N} = \mathbf{T}^+_{k_0-M,\ell_0+M,N} = \mathbf{I}$$

disappears after a finite number of steps, denoted by $\hat{n}$, where $\mathbf{I}$ stands for an identity matrix of dimensions $(2N+1) \times (2N+1)$. Then, for $n \geq \hat{n}$ the recursion for $\mathbf{T}_{k_{n+1}-M,\ell_{n+1}+M,N}$, and thereby its pseudo inverse $\mathbf{T}^+_{k_{n+1}-M,\ell_{n+1}+M,N}$ becomes accurate. This method was confirmed by simulations. After the disappearance of the initial errors the same error function was obtained as that shown in Figure 7 for $N = 8$ We note that for large N the method exhibits sensitivity to the order of the consecutive subtractions and additions of $\mathbf{u}_i \mathbf{u}_i^H$.

2.6 Reconstruction by Using FFT

If further evaluation using digital signal processing is needed on the reconstructed signal, it has to be sampled uniformly. We show that under mild conditions the uniformly-taken samples can be calculated efficiently via FFT. Denoting the sampling period by T_s, the reconstruction in (25) becomes:

$$x_{M,N}(kT_s) = \sum_{n\in\mathbb{Z}} w(kT_s - nT_0) D(M,N)_{k,n}$$

where:

$$D(M,N)_{k,n} = \sum_{m=-N}^{N} d(M,N)_{m,n} e^{jm\frac{\Omega}{N}kT_s}. \tag{29}$$

Denoting the Nyquist period of $x(t)$ by T ($\Omega = \pi/T$) and with appropriate positive integers N_w, N_0, and N_s assuming

$$T_w = N_w T_s, \quad T_0 = N_0 T_s \quad \text{and} \quad T = N_s T_s \tag{30}$$

we have:

$$x_{M,N}(kT_s) = \sum_{n\in\mathbb{Z}} w(kT_s - nN_0T_s) D(M,N)_{k,n} \tag{31}$$

Since $w(t) \neq 0$ holds only for $-T_w \leq t \leq T_w$, $w(kT_s - nN_0T_s) \neq 0$ only when $-T_w \leq kT_s - nN_0T_s \leq T_w$ or equivalently (see (30)) when $N_w + k \leq nN_0 \leq -N_w + k$ holds. Therefore, (31) becomes:

$$x_{M,N}(kT_s) = \sum_{n=\lceil\frac{k-N_w}{N_0}\rceil}^{\lfloor\frac{k+N_w}{N_0}\rfloor} w(kT_s - nN_0T_s) D(M,N)_{k,n} \tag{32}$$

Rewriting $D(M,N)_{k,n}$ in (29) gives:

$$D(M,N)_{k,n} = e^{-j\Omega kT_s} \sum_{\ell=0}^{2N} d(M,N)_{\ell-N,n} e^{j\ell\frac{\Omega}{N}kT_s}.$$

Using (30) and the familiar notation

$$W_K = e^{j\frac{2\pi}{K}}$$

gives:

$$D(M,N)_{k,n} = W_{2N_s}^{-k} \sum_{\ell=0}^{2N} d(M,N)_{\ell-N,n} W_{2NN_s}^{\ell k}$$

Since the bandwidth of the reconstructed signal is greater than Ω (see Section 2.4) $T_s < T$ certainly holds. Then, however, $N_s > 1$, and thereby $2NN_s > 2N+1$ also holds. Therefore, with the zero-padded sequence

$$h(M,N)_{\ell,n} = \begin{cases} d(M,N)_{\ell-N,n} & \text{if} \quad \ell \in [0,2N] \\ 0 & \text{if} \quad \ell \in (2N, 2NN_s - 1] \end{cases} \tag{33}$$

we have

$$D(M,N)_{k,n} = W_{2N_s}^{-k} \sum_{\ell=0}^{2NN_s-1} h(M,N)_{\ell,n} W_{2NN_s}^{\ell k}. \tag{34}$$

The summation in (34) can directly be calculated by using FFT.

3 Conclusions and Future Work

We summarize some of the potentials of the proposed method.

- Since apart from the partition-of-unity requirement no constrains are imposed on the window functions $w(t)$, several scaling functions used in the theory of Wavelets, e.g. [3], can be tested and compared in terms of accuracy, computational complexity, and insensitivity to finite-precision arithmetic. Our immediate goal is to consider orthogonal scaling functions.

- Note that the reconstruction in (25) is essentially a Gabor-system representation of $x(t)$, see e.g. [6, 3]. Our goal is to investigate Gaussian windows when Gabor systems become Gabor frames. Although Gaussian windows are not compactly supported, they might have other advantages.

- The key formula in (26) for pseudo-inverse recursion does not take advantage of the fact that we are dealing Hermitian Toeplitz matrices. Our goal is to simplify the recursion in Section 2.5 by taking this property into account.

References

[1] S. L. Campbell and C. D. Meyer Jr., *Generalized Inverses of Linear Transformations*, Dover Publications, 1979.

[2] O. Christensen, "Frames Riesz Basis, and Discrete Gabor/Wavelet Expansions", Bulletin (New York) of the American Mathematical Society, Vol. 38, No. 3, pp. 273-291, March 27, 2001.

[3] I. Daubechies, "The wavelet transform, time-frequency localization and signal analysis", IEEE Transactions on Information Theory, Vol. 36, No. 5., pp. 961-1005, September 1990.

[4] H. G. Feichtinger and K. Gröchenig, "Theory and Practice of Irregular Sampling". In J.J. Benedetto and M.W. Frazier, editors, Wavelets: Mathematics and Applications, pp. 305-363, CRC Press, Boca Raton, FL, 1994.

[5] H. G. Feichtinger, K. Grochenig, and T. Strohmer: "Efficient numerical methods in non-uniform sampling theory", Numerische Mathematik, 69:423-440, 1995.

[6] D. Gabor, "Theory of communications", J. Inst. Electr. Eng. (London), Vol. 93, No. III, pp. 429-457, 1946.

[7] C. J. Kikkert, and D. J. Miller, "Asynchronous delta sigma modulation", Proceedings of the IREE (Australia), Vol. 36, pp. 83-88, April 1975.

[8] J. Kovačević, P.L. Dragotti, V.K. Goyal, "Filter Bank Frame Expansions with Erasures", IEEE Transactions on Information Theory, Vol. 48, No. 6 pp. 1439-1450, June 2002.

[9] A.A. Lazar and L.T. Tóth, "Time Encoding and Perfect Recovery of Bandlimited Signals", Proceedings of the ICASSP'03, Vol. VI, pp. 709-712, April 6-10 2003, Hong Kong.

[10] A.A. Lazar, "Time Encoding with an Integrate-and fire Neuron with a Refractory Period", Neurocomputing, Vol. 58-60, pp. 53- 58, 2004.

[11] A.A. Lazar and L.T. Tóth, "Perfect Recovery and Sensitivity Analysis of Time Encoded Bandlimited Signals", IEEE Transactions on Circuits and Systems-I: Regular Papers, Vol. 51, No. 10, pp. 2060-2073, October 2004.

[12] A.A. Lazar, E. K. Simonyi, and L. T. Tóth, "Fast recovery algorithms of time encoded bandlimited signals," Proceeding of the International Conference on Acoustics, Speech and Signal Processing (ICASSP'05), Philadelphia, PA, March 19-23, 2005, Vol. 4, pp. 237-240, 2005.

[13] A.A. Lazar, E. K. Simonyi, and L.T. Tóth, "A real-time algorithm for time decoding machines," BNET Technical Report #4-05, Department of Electrical Engineering, Columbia University, New York, October 2005.

[14] E. Roza, "Analog-to-digital conversion via duty-cycle modulation", IEEE Transactions on Circuits and Systems-II: Analog and Digital Signal Processing, Vol. 44, No. 11, pp. 907-917, November 1997.

[15] T. Strohmer, *Irregular Sampling, Frames, and Pseudoinverse*, Master thesis, Dep. Math. Univ. Vienna, Austria, 1993.

[16] M. Unser and T. Blu, "Wavelet theory demystified", IEEE Transactions on Signal Processing, Vol. 51, No. 2, pp. 470-483, February 2003.